vol. 173, no. 3 the american naturalist march 2009

E-Article

Diversity and Composition of Viral Communities: Coinfection of Barley and Cereal Yellow Dwarf Viruses in California Grasslands

Eric W. Seabloom,[1,*,†] Parviez R. Hosseini,[2,†] Alison G. Power,[3] and Elizabeth T. Borer[1]

1. Department of Zoology, Oregon State University, Corvallis, Oregon 97331; 2. Department of Ecology and Evolutionary Biology, Princeton University, Princeton, New Jersey 08544; 3. Department of Ecology and Evolutionary Biology, Cornell University, Ithaca, New York 14853

Submitted November 2, 2007; Accepted July 7, 2008; Electronically published January 30, 2009

abstract: Most species host multiple pathogens, yet field studies rarely examine the processes determining pathogen diversity within a single host or the effects of coinfection on pathogen dynamics in natural systems. Coinfection can affect pathogen transmission and virulence. In turn, coinfection can be regulated within hosts by interactions such as cross-protective immunity or at broader spatial scales via vector distributions. Using a general model, we demonstrate that coinfection by a group of vectored pathogens is highest with abundant generalist vectors and weak cross-protection and coinfection-induced mortality. Using these predictions, we investigate the distribution of five coexisting aphid-vectored, viral pathogens (barley and cereal yellow dwarf luteoviruses and poleroviruses) in a native perennial grass (*Elymus glaucus*) in both space (700 km) and time (4 years). Observed coinfection rates were much higher than expected at random, suggesting that within-host processes exerted weak effects on within-host pathogen diversity. Covariance among viruses in space and time was highest for viral species sharing a vector. Temporal correlation arose from the synchronous invasion of two viruses transmitted by a shared aphid species. On the basis of our modeling and empirical results, we expect that factors external to individual hosts may affect the coinfection dynamics in other communities hosting vectored pathogens.

Keywords: disease ecology, viral pathogen, aphid, vector, interference, positive interaction, facilitation.

Introduction

Most species are hosts to multiple pathogens (Lello et al. 2004; Jolles et al. 2008), and in many cases, individual hosts are simultaneously infected by multiple pathogens or pathogen strains, also termed "coinfected." Coinfection can have strong impacts on pathogen dynamics by altering processes such as pathogen transmission and host mortality (Rochow 1970*b*; Creamer and Falk 1990; Miller and Rasochova 1997; Thomas et al. 2003; Rohani et al. 2003; Lello et al. 2004; Koskella et al. 2006; Pedersen and Fenton 2007). Coinfection can be mediated by direct pathogen-pathogen interactions within a host, host immune responses, or even vector ecology and community composition (Power et al. 1991; Dempster and Holmes 1995; Power 1996). While the importance of among-pathogen interactions is gaining increasing recognition in human and agricultural systems (e.g., Zhang and Holt 2001; Rohani et al. 2003; Huang and Rohani 2005), few field studies have examined the processes governing coinfection and its impacts on pathogen diversity and infection prevalence in naturally occurring host populations (Hood 2003; Lello et al. 2004; Koskella et al. 2006; Jolles et al. 2008).

Pathogen interactions can increase transmission rates via a variety of processes. For example, a primary infection can lower host resistance to subsequently invading pathogens (Bentwich et al. 1999; Koskella et al. 2006), as in immunodeficiency syndromes such as AIDS or in organisms with cross-regulation between immune systems for micro- and macroparasites (Bentwich et al. 1999; Yazdanbakhsh et al. 2002; Coico et al. 2003; Jolles et al. 2008). Transmission rates of viral pathogens also may be higher in coinfected hosts as a result of antibody-dependent enhancement, in which exposure to one virus increases the replication rate of a second invading virus, exemplified by human immunodeficiency viruses (e.g., Montefiori et al. 1996; Tirado and Yoon 2003). For vectored viral pathogens, heterologous encapsidation (i.e., transcapsidation), in which the genome of one virus is encased within the protein coat of a different coreplicating virus, may allow efficient transmission by novel vectors (Rochow 1970*b*; Creamer and Falk 1990). Thus, coinfected hosts might act as superspreaders by providing higher than expected transmission rates (Woolhouse et al. 1997).

Conversely, pathogen interactions can lower transmis-

* Corresponding author; e-mail: seabloom@science.oregonstate.edu.
† Contributed equally to manuscript.

Am. Nat. 2009. Vol. 173, pp. E79–E98.
0003-0147/2009/17303-50040$15.00.
DOI: 10.1086/596529

sion by decreasing vector efficiency, viral titers, or sporulation in coinfected hosts (Gildow and Rochow 1980; Gray et al. 1991; Wen et al. 1991; Power 1996; Al-Naimi et al. 2005). Within-host processes, such as immune system upregulation in coinfected hosts, may limit the ability of hosts to acquire new infections (Durrant and Dong 2004). Closely related pathogens may provide a degree of cross-protection, providing vaccinelike protection (Rochow 1970*b*). Altered behavioral patterns in infected hosts also may limit exposure of infected individuals to novel pathogens (Huang and Rohani 2005).

Coinfection can lead to increased virulence (e.g., increased host mortality or lowered fecundity), as is the case for humans coinfected by multiple human immunodeficiency viral strains, hepatitis C virus and the trematode *Schistosoma mansoni*, or human immunodeficiency virus and malaria (Lal et al. 1994; Kamal et al. 2001*a*, 2001*b*; Tirado and Yoon 2003), leading to reduced transmission at the level of the host population. Increased mortality of coinfected hosts is also a common phenomenon in plants infected with multiple RNA viral or fungal pathogens (Miller and Rasochova 1997; Hood 2003).

Coinfection rates are not necessarily driven by within-host interactions; they can be governed by processes that act at broad spatial scales, including vector movement and climatic variability (Dempster and Holmes 1995; Power 1996). Factors controlling the vector community, such as climate or habitat suitability, also may control the occurrence of infection and coinfection in the host community (Cumming and Guegan 2006; Knols and Louis 2006; Alto et al. 2008). Finally, spatial and temporal factors controlling host community composition may affect the likelihood of coinfection within individual hosts, although this has been little explored.

The need for a general exploration of the causes and consequences of coinfection is suggested by the observations that coinfection is common in both animal and plant hosts, governed by many processes both within and external to hosts, and can have dramatic consequences for both hosts and pathogens. Here, we begin by developing a susceptible-infected (SI) model with two pathogen taxa. We explicitly include cross-protective immunity and allow transmission and host mortality to differ among uninfected, singly infected, and coinfected hosts. We also explicitly incorporate vector abundance and allow vector efficiency to vary for the different pathogens. We use the model to make qualitative and quantitative predictions about the influence of these factors on both coinfection and on the proportion of the total host population infected by at least one of the pathogen taxa (prevalence).

Motivated by these theoretical predictions, we then examine the spatial and temporal patterns of coinfection rates in a suite of five generalist RNA luteoviruses and poleroviruses referred to collectively as barley and cereal yellow dwarf viruses (B/CYDVs). We track the distribution and diversity of these viruses in restored and natural grassland communities in California across spatial (700 km), rainfall (380–620 mm), and temporal (4 years) gradients. Using data on B/CYDV infections in a native grass host, we test whether overall coinfection rates by the five viruses differ from that expected under a random distribution, then we test whether spatial and/or temporal covariance of the viral species is consistent with model predictions.

Study System

B/CYDV and Invasion in California Grasslands

California's grasslands are of great conservation interest as both a global biodiversity hotspot and the site of one of the most dramatic and persistent plant invasions worldwide. The California flora contains about 20% of the vascular flora in the United States and 4% worldwide, and about 30% of the these species are California endemics (Stein et al. 2000; Seabloom et al. 2002). While originally dominated by native perennial species, exotic annual species have dominated almost all of this state's 9 million hectares of grasslands for more than a century (Heady 1977; D'Antonio and Vitousek 1992; Mensing and Byrne 1998).

Recently, B/CYDV has been implicated as a factor likely to have mediated the invasion and sustained dominance by these exotic grasses (Malmstrom et al. 2005*a*; Borer et al. 2007). In the absence of B/CYDV, native perennial grasses are competitively dominant and are able to exclude exotic annual grasses. However, the presence of exotic annuals increases B/CYDV prevalence and lowers the competitive ability of the native perennial species, allowing coexistence of exotic annual and native perennial species (Malmstrom et al. 2006; Borer et al. 2007).

Barley and Cereal Yellow Dwarf Viruses

B/CYDVs are a group of aphid-vectored, RNA luteoviruses and poleroviruses that are responsible for one of the most economically devastating diseases of grasses worldwide and one of the most prevalent of all viral diseases (Irwin and Thresh 1990; D'Arcy 1995). These viruses affect more than 150 hosts, including cereal crops, forage crops, naturalized exotic grasses, and native grasses (D'Arcy 1995). B/CYDV infection commonly causes stunting of stems and roots, lowered fecundity, and increased mortality (Rochow 1970*a*; D'Arcy 1995; Jensen and D'Arcy 1995; Malmstrom et al. 2005*b*). Symptoms may be expressed within 1–14 days (i.e., latency period), depending on temperature; however, the virus moves rapidly through the phloem, and

new vectors can acquire the disease within 5 h of infection (Agrios 1988).

B/CYDVs are obligately aphid vectored, and at least 25 aphid species in six different genera have been documented as vectors (Halbert and Voegtlin 1995). There is no vertical transmission of B/CYDVs across host generations via seed or direct transmission from infected to uninfected hosts (Rochow 1970*a*). B/CYDVs are circulative (persistent) viruses, accumulating internally within the aphid vector (Rochow 1970*a*). Aphid vectors do not pass the viruses to their offspring, and the virus does not replicate within the vectors (Agrios 1988; Rochow 1970*a*). Vectors differ widely in their efficiency at transmitting different viral species, with efficiency likely governed by the protein coat of the virus (Miller and Rasochova 1997). Viral acquisition by aphids and inoculation of hosts is rapid. Aphids can acquire the virus after feeding on infected plants for as little as 15 min, though efficient transmission (>50%) requires acquisition periods of up to 3 h (Gray et al. 1991). Viruliferous aphids can inoculate host plants after feeding for 30 min; however, efficient transmission (>50%) requires inoculation periods of 2 h to 3 days, depending on the aphid species (Power et al. 1991).

The B/CYDVs are divided into two genera: (1) the barley yellow dwarf viruses (BYDVs) and (2) the cereal yellow dwarf viruses (CYDVs; table 1; Miller and Rasochova 1997; Malmstrom and Shu 2004). The genetic differences between the BYDV and the CYDV groups are very pronounced. Genetically, BYDVs more closely resemble soybean dwarf luteovirus than do CYDVs, and CYDVs more closely resemble beet western yellows and potato leafroll luteoviruses than do BYDVs (Miller and Rasochova 1997). The viruses differ in their virulence, with the widespread BYDV-PAV typically having the most severe effects on hosts (Miller and Rasochova 1997).

This suite of viruses is particularly well suited for examining the effects of coinfection on pathogen dynamics, because there is strong empirical evidence that coinfection by multiple B/CYDV species can alter cross-protection, host mortality, and transmission rates in predictable ways. Cross-protection occurs among BYDV species (BYDV-PAV and BYDV-MAV), although there is no evidence of cross-protection among the CYDVs or between the two viral groups (Wen et al. 1991; Miller and Rasochova 1997). Infections by viruses from different groups (e.g., BYDV-PAV and CYDV-RPV) can increase virulence, as is the case with most luteoviruses (Miller and Rasochova 1997), and potentially increase host mortality. Finally, aphid vectors differ in their transmission efficiency for each virus, and coinfection can increase transmission by less efficient vectors (Power and Gray 1995).

The most common B/CYDV vectors at our study sites are *Rhopalosiphum padi*, *Rhopalosiphum maidis*, *Sitobion avenae*, *Metopolophium dirhodum*, and *Schizaphis graminum* (E. T. Borer, unpublished data). Of these species, *R. maidis* and *S. graminum* each efficiently vector only a single viral species (BYDV-RMV and BYDV-SGV, respectively). In contrast, *R. padi* is an efficient vector for both BYDV-PAV and CYDV-RPV. Similarly, *S. avenae* and *M. dirhodum* efficiently transmit two BYDV species (BYDV-PAV and BYDV-MAV; table 1; Power and Gray 1995; Miller and Rasochova 1997; Leclercq-Le Quillec et al. 2000).

Table 1: Barley and cereal yellow dwarf virus (B/CYDV) serotypes, subgroups, genera, and their major vectors

Serotype	Subgroup	Genus	Rp	Rm	Sa	Md	Sg
SGV	I BYDV	Unassigned					X
MAV	I BYDV	*Luteovirus*			X	X	
PAV	I BYDV	*Luteovirus*	X		X	X	
RPV	II CYDV	*Polerovirus*	X				
RMV	II CYDV	Unassigned		X			

Note: *Rhopalosiphum padi* (Rp), *Rhopalosiphum maidis* (Rm), *Sitobion avenae* (Sa), *Metopolophium dirhodum* (Md), and *Schizaphis graminum* (Sg; Power and Gray 1995; Miller and Rasochova 1997; Leclercq-Le Quillec et al. 2000).

General Model of Coinfection

Modeling Framework

We developed a model to explore the general implications of coinfection rates, given the empirical evidence that coinfections can change both virulence and transmission. We use this model to determine whether and when vectors, cross-protection, and synergistic mortality produce detectable responses across a gradient of pathogen relatedness. We examine a system in which two vectored pathogen taxa (A and B) can infect a single host. The host can exist in one of four states: uninfected by either pathogen (S), infected by pathogen A (I_A), infected by pathogen B (I_B), or infected by both A and B ($I_{A,B}$).

In order to match the biology of our B/CYDV case study, we will focus primarily on the interactions between two pathogen taxa in which the distinctiveness of these taxa determines both cross-protection and synergistic mortality (ψ). Specifically, our model reflects a trade-off found in many RNA viral systems (e.g., B/CYDVs) in which very similar viruses ($\psi \to 0$) provide high levels of cross-protection and cause little synergistic mortality, while highly distinct viruses ($\psi \to 1$) impart no added protection and coinfection can cause increased host mortality (cf. May and Nowak 1995). We also discuss the general effects of decoupling cross-protection and synergistic virulence, as in systems with cross-protection between very different types of pathogens (e.g., viral and fungal), through mech-

anisms such as systemic acquired resistance (Durrant and Dong 2004).

The dynamics of this system can be described using the following set of differential equations:

$$\frac{dS}{dt} = -\beta_V V_A S - \beta_V V_B S - \mu_0 S + [b_S S + b_1(I_A + I_B) + b_2 I_{A,B}]\left(1 - \frac{N}{K}\right), \quad (1)$$

$$\frac{dI_A}{dt} = \beta_V V_A S - \beta_V \psi V_B I_A - (\mu_0 + \mu_1) I_A, \quad (2)$$

$$\frac{dI_B}{dt} = \beta_V V_B S - \beta_V \psi V_A I_B - (\mu_0 + \mu_1) I_B, \quad (3)$$

$$\frac{dI_{A,B}}{dt} = \beta_V \psi (V_B I_A + V_A I_B) - (\mu_0 + \mu_1 + \psi\mu_2) I_{A,B}, \quad (4)$$

where μ_0, μ_1, and μ_2 are the incremental death rates for plants infected by no pathogens, one pathogen taxa, and both pathogen taxa, respectively; N is total host density ($S + I_A + I_B + I_{A,B}$); and K is the host carrying capacity. Transmission rates in this system are a function of the transmission rate from vectors to plants (β_V), the proportional reduction in transmission to previously infected hosts due to cross-protection (ψ), and the frequency of pathogen-carrying vectors, defined here as

$$V_A = \frac{\beta_{X,A}(I_A + I_{A,B})}{\beta_{X,A}(I_A + I_{A,B}) + \beta_{X,B}(I_B + I_{A,B}) + \delta} X + \frac{\beta_{Y,A}(I_A + I_{A,B})}{\beta_{Y,A}(I_A + I_{A,B}) + \beta_{Y,B}(I_B + I_{A,B}) + \delta} Y, \quad (5)$$

$$V_B = \frac{\beta_{X,B}(I_B + I_{A,B})}{\beta_{X,A}(I_A + I_{A,B}) + \beta_{X,B}(I_B + I_{A,B}) + \delta} X + \frac{\beta_{Y,B}(I_B + I_{A,B})}{\beta_{Y,A}(I_A + I_{A,B}) + \beta_{Y,B}(I_B + I_{A,B}) + \delta} Y, \quad (6)$$

where X and Y are the total abundances of two distinct vector species and V_A and V_B are the total numbers of vectors (of either species) carrying pathogen A or pathogen B. The term $\beta_{Z,C}$ is the transmission rate of pathogen C when carried by vector species Z. These formulas are based on a pseudoequilibrium argument (app. B). We can use this model to explore the effects of vector specificity by comparing cases in which vectors carry a single pathogen taxa ($\beta_{X,B} = \beta_{Y,A} = 0$) or where vectors are generalists and can carry multiple pathogen taxa ($\beta_{X,B} > 0$ and $\beta_{Y,A} > 0$). We have not included a latent period in our model, since B/CYDV can be both acquired and transmitted rapidly (Gray et al. 1991; Power et al. 1991). While a short latent period could be included through an additional parameter in the denominator of our vector equations, the separation of timescales that underlies a pseudoequilibrium argument could be much more problematic for long latent periods, particularly in a case such as malaria (MacDonald 1957).

Most model parameters, found in table A1, were based on field estimates from Seabloom et al. (2003) and Malmstrom et al. (2005*b*) and as calculated by Borer et al. (2007). However, Borer et al. (2007) did not use the aphid transmission model developed here or focus on coinfection, so these transmission parameters were estimated separately. Aphid life span is up to a month (E. T. Borer, unpublished data), which gives us an estimate for δ. To examine synergistic mortality, we assume that mortality was additive ($\mu_1 = \mu_2$), which comports with anecdotal evidence (Miller and Rasochova 1997; fig. 1*B*); we examine and relax this assumption in appendix A. Because the dynamics of aphid virus acquisition and transmission are broadly similar for B/CYDV (Gray et al. 1991; Power et al. 1991), we have estimated all transmission parameters with the same value but kept the names distinct for clarity of discussion and because some can be set to zero for the specialist vector scenario. We select our transmission parameter estimates largely by matching field prevalence, given all realistic estimates of other parameters.

Modeling Results

Generalist vectors (e.g., *Rhopalosiphum padi*, *Sitobion avenae*, and *Metopolophium dirhodum* in our system) lead to more coinfection in the host population than do specialist vectors (fig. 1*B*; fig. 2*A*, 2*C*; fig. 3), and individual strains carried by generalist vectors tend to covary positively (fig. 2*A*, 2*C*). Specialist vectors (e.g., *Rhopalosiphum maidis* and *Schizaphis graminum* in our system) produce a more complex picture. Singly infected hosts may covary negatively in the population while still producing a fair to substantial level of coinfection, which will create an overall positive, yet weak, covariance (fig. 2*A*, 2*C*). The degree of vector specialization has a decreasing impact on overall infection prevalence as transmission rates increase. Total disease prevalence is highest for abundant, generalist vectors (fig. 1*A*). Increasing specialist vector abundance always increases the prevalence of the strain it carries, while increasing generalist vector abundance can actually decrease solitary strain prevalence (fig. 2). Intriguingly, increasing specialist vector abundance decreases the nonvectored strain's overall prevalence (i.e., for increasing X, which increases $I_A + I_{A,B}$, $I_B + I_{A,B}$ decreases; fig. 2*B*, 2*D*; fig. 3*A*, 3*C*). Thus, one can find slight decreases in total disease prevalence as a result of synergistic mortality of

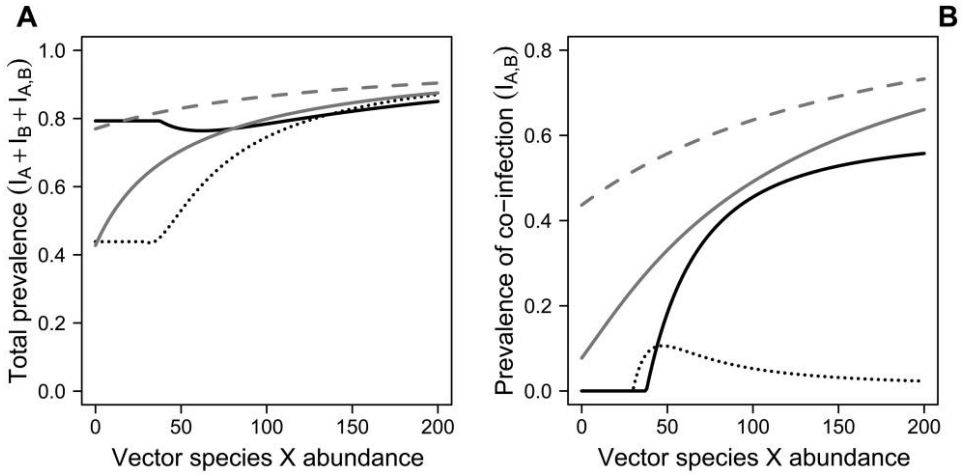

Figure 1: Total disease prevalence (*A*) and prevalence of coinfections (*B*) as a function of vector *X* abundance. Solid black line represents two specialist vectors with $Y = 120$, dashed gray line represents two generalist vectors with $Y = 120$, dotted black line represents two specialist vectors with $Y = 40$, and solid gray line represents two generalist vectors with $Y = 40$. All other parameters as in table A1.

coinfected individuals for certain levels of specialist vector abundances (fig. 1), but this seems to be a relatively rare and minor phenomenon. Coinfection for specialist vectors alone is greater either with high vector evenness ($X \approx Y \approx 40$; fig. 2*B*) or when both vectors are very abundant ($X, Y > 120$; fig. 2*D*).

In mixed communities of specialist and generalist vectors, increasing specialist vector abundance increases the prevalence of the strain it carries while decreasing the prevalence of the other strain. In these mixed communities, the rate of coinfection either remains relatively constant or decreases, depending on the abundance of generalist vectors (fig. 3*A*, 3*C*). Increasing generalist vector abundance increases prevalence of coinfections and the strain that is not carried by the specialist, once a threshold abundance of generalist vectors is reached; below this threshold, generalist vectors only add to the spread of the strain carried by the specialist (fig. 3*B*, 3*D*). This threshold abundance for invasion of a second strain into the system is higher than the abundance necessary for a single strain to spread into the system (fig. 2*B*, 2*D*; fig. 3*B*, 3*D*). Thus, although synergistic mortality has minor effects on overall disease prevalence, in the case of specialist vectors it can allow for competitive displacement of one strain by another, but not in the case of generalist vectors. More broadly, this result demonstrates how vector community composition (relative abundance and degree of specialization) can strongly control virus community composition and coinfection rates in hosts and thus overall disease prevalence.

Parameterized for the B/CYDV system, pathogen taxa similarity has a minor effect on overall pathogen prevalence; transmission rate (β), unsurprisingly, substantially impacts overall infection (fig. 4*A*). Vector specialization also affects prevalence; generalist vectors favor more similar pathogen taxa than specialist vectors, particularly when disease transmission is high (fig. 4*A*). In contrast, the increase in disease prevalence at moderate levels of ψ occurs despite a monotonic decline in singly infected hosts. The drop in singly infected hosts is overwhelmed by the rise in coinfected hosts, except when coinfection causes substantial synergistic mortality ($\mu_2 \gg 0$), but there is no additional mortality on singly infected hosts ($\mu_1 = 0$; figs. A1, A2). In contrast, as cross-protection declines ($\psi \to 1$), coinfection prevalence increases monotonically over a wide range of transmission rates (β). Coinfection is strongly suppressed by cross-protection when pathogen taxa are very similar but increases rapidly as species diverge. Synergistic mortality limits but does not prevent the occurrence of hosts infected with dissimilar pathogen taxa. Thus, these model results suggest that similar pathogen taxa should not co-occur in hosts, but distinct pathogen taxa may be present at relatively high rates, depending on transmission (fig. 4*B*).

In summary, this modeling exercise leaves us with the following testable predictions for examining a field system. (1) High levels of coinfection occur when there are abundant, generalist vectors that carry multiple pathogen taxa and when there are no among-strain interactions (i.e., no cross-protection or synergistic mortality). In contrast, increasing levels of vector specialization, cross-protection, and synergistic mortality will reduce coinfection rates. We test for the overall importance of within-host processes by determining whether coinfection rates of B/CYDV species

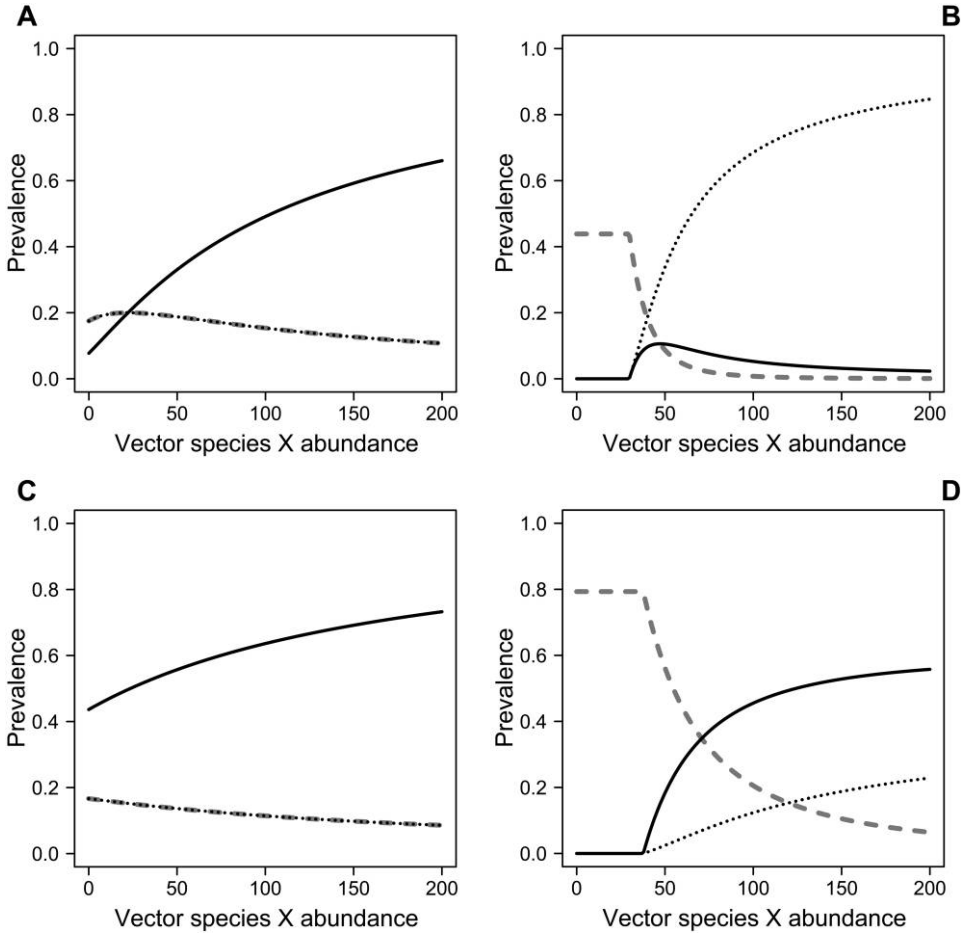

Figure 2: Prevalence of infections with strain A (*dotted black line*), strain B (*dashed gray line*), and coinfections (*solid black line*) as a function of vector *X* abundance. *A*, Both vectors are generalists, $Y = 40$. *B*, Both vectors are specialists, $Y = 40$. *C*, Both vectors are generalists, $Y = 120$. *D*, Both vectors are specialists, $Y = 120$. Other parameters as in table A1.

are higher than expected in our empirical data. (2) Pathogen taxa carried by generalist vectors should covary positively more than those carried by specialists. The model produced a strong vector signal that should be evident even in field data. We test the importance of vector generality by determining whether B/CYDV species that share a vector are more positively correlated than expected at random among sites and years. (3) Increasing levels of cross-protection will reduce coinfection, whereas increasing levels of synergistic mortality will reduce overall prevalence weakly. Thus, when examining rates of coinfection in the field, we should expect to find greater coinfection by dissimilar B/CYDV species because of cross-protection but little effect of synergistic mortality on coinfection rates. Notably, within-host processes produced negative covariance within viral groups, whereas generalist vectors caused positive covariance among viruses they carry, regardless of viral similarity. We test the importance of within-host processes by determining whether B/CYDV species within a viral group are more negatively correlated than expected at random among sites and years.

Empirical Methods

Sampling Design

We measured the prevalence of five species of B/CYDV in the native perennial grass *Elymus glaucus* in restored and natural grasslands in California. We selected *E. glaucus* because it is one of the most widespread of the native western grasses and is common in grasslands from Mexico to Canada. The extensive range of this species allows us to make large-scale geographic comparisons among individual hosts of the same species.

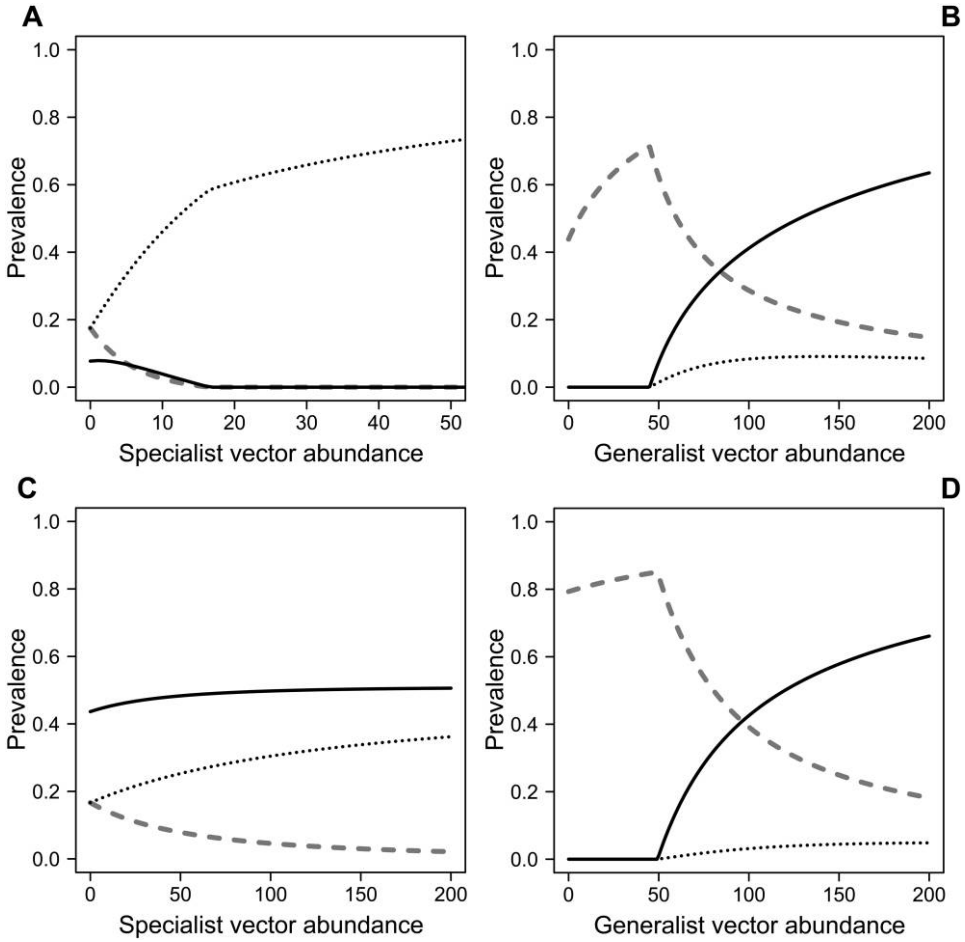

Figure 3: Prevalence of infections with strain A (*dotted black line*), strain B (*dashed gray line*), and coinfections (*solid black line*) as a function of vector *X* abundance, with one specialist and one generalist vector. *A*, Generalist abundance fixed at 40, specialist vector abundance varying. *B*, Specialist abundance fixed at 40, generalist vector abundance varying. *C*, Generalist abundance fixed at 120, specialist vector abundance varying. *D*, Specialist abundance fixed at 120, generalist vector abundance varying. Other parameters as in table A1. Note that the *X*-axis in *A* has been shortened to match the region over which the strains' prevalences change.

We monitored B/CYDV at three reserves within the University of California Natural Reserve System: Sedgwick Reserve (34°40′21″N, 120°00′33″W), Hastings Natural History Reservation (36°23′17″N, 121°32′60″W), and McLaughlin Natural Reserve (38°52′26″N, 122°25′54″W). These sites represent roughly a twofold variation in rainfall from 380 mm at the southern site (Sedgwick) to 620 mm at the northern site (McLaughlin). Our sampling occurred during a particularly wet year that resulted in an unusual ordering of rainfall: south (Sedgwick, 1,194 mm), north (McLaughlin, 1,007 mm), and central (Hastings, 638 mm). These sites are located in oak savanna habitat and have a Mediterranean climate typified by hot dry summers (mean summer high 32°–34°C) and cool wet winters (mean winter high 12°–13°C).

We compared spatial variability in the viral community by selecting three isolated populations of *E. glaucus* at each reserve. *Elymus glaucus* has a very patchy distribution at these reserves, since it is typically found under oak canopies, that can be quite isolated in these savanna habitats. The populations used in our sampling were separated by at least 500 m and were of comparable size and community composition. We collected leaves from 10 individual plants in each of nine *E. glaucus* populations in the spring of 2005.

We compared temporal variability of the viral community in *E. glaucus* in a restored grassland from 2002 to 2005 at our southern site (Sedgwick Reserve). This grassland was planted to native perennial grasses in 1998 (for more details, see Seabloom et al. 2003). Rainfall was quite

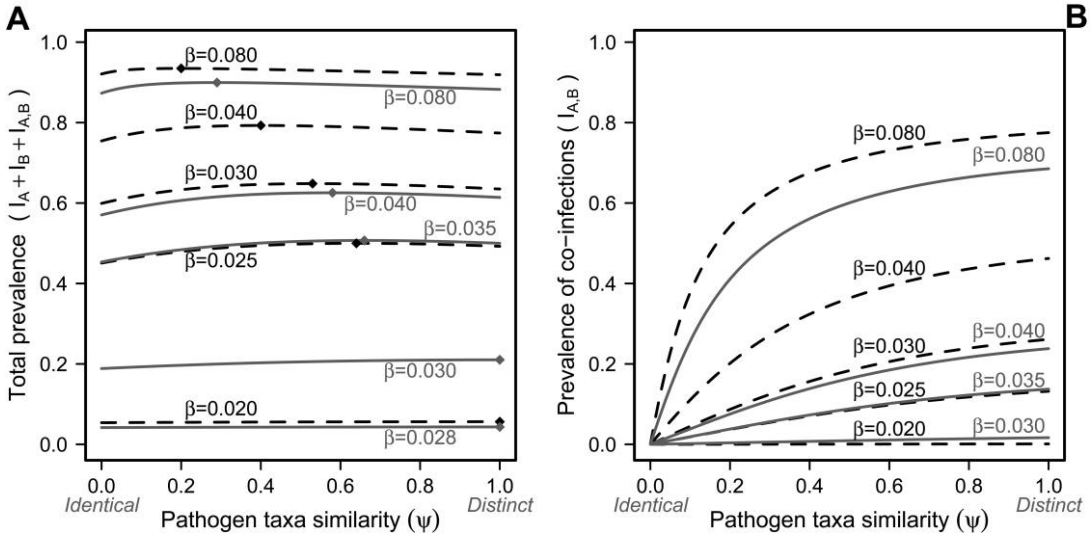

Figure 4: Total disease prevalence (*A*) and prevalence of coinfections (*B*) for various values of β as a function of the level of cross-protection ($1 - \psi$). Solid gray lines represent specialist vectors ($X = 50$, $Y = 50$), dashed black lines represent generalist vectors ($X = 100$, $Y = 0$). In *A*, circles represent peak prevalence for a given β. Other parameters as in table A1. For a full display of continuous parameter space, see appendix A.

variable during this period, with growing season (July to July) rainfall as follows: 2002, 221 mm; 2003, 503 mm; 2004, 263 mm; and 2005, 1,194 mm. We collected leaves from 10 *E. glaucus* plants from each of 10 replicate 3 × 3-m plots in each year at peak biomass.

Viral Assays

Leaf tissue from each host was tested for infection by any B/CYDV virus (BYDV-PAV, BYDV-MAV, BYDV-SGV, CYDV-RPV, and CYDV-RMV) using the double antibody sandwich enzyme-linked immunosorbent assay (DAS-ELISA) using antibodies provided by S. Gray (Cornell University, Ithaca, NY) and Agdia (Elkhart, IN; Rochow 1986). We used reference controls of closely related viruses and species on each ELISA plate to screen out any misleading cross-reactions.

Statistical Analyses

We used Mantel tests to look for association between the 5 × 5 correlation matrix of the B/CYDV viral species and two 5 × 5 design matrices that distinguished between viral species that occur in the same group or are carried by the same vector (table 1). We constructed the first design matrix **G** to test whether viruses in the same group had lower correlations (as a result of cross-protection) than expected at random. In this matrix, viral species in the same group (e.g., BYDV) had a distance of 0, and species in different groups were assigned a value of 1. Specifically,

$$\mathbf{G}_{ij} = \begin{cases} 0 & \text{if } i \text{ and } j \text{ are species in the same group} \\ 1 & \text{otherwise} \end{cases}. \tag{7}$$

Similarly, we constructed a design matrix **V** that tested whether viruses carried by the same vector were more highly correlated than expected at random. In this matrix, viral species carried by the same vector had a value of 1, and species carried by different vectors were assigned a value of 0. Specifically,

$$\mathbf{V}_{ij} = \begin{cases} 1 & \text{if species } i \text{ and } j \text{ share a vector} \\ 0 & \text{otherwise} \end{cases}. \tag{8}$$

We also tested for the species-specific effects of the vectors that carry multiple viral species (*Rhopalosiphum padi* and *Sitobion avenae*/*Metopolophium dirhodum*) using two design matrices that are slight variants of **V**. One of these matrices tested for positive correlations only among *R. padi* vectored viruses (BYDV-PAV and CYDV-RPV), and the other tested for correlations among the *S. avenae*/*M. dirhodum* vectored viruses (BYDV-PAV and BYDV-MAV).

In our tests, we used the standardized Mantel statistic *Z*, the product moment correlation coefficient (*r*) between the corresponding elements in two matrices. As with the familiar correlation coefficient, *Z* ranges from −1 to 1. In our analysis, large positive values of *Z* indicate that the viral community is more similar within categories in the design matrix than among categories. We tested the sig-

nificance of Z by comparing the calculated value to the distribution of values obtained in 999 random permutations of the viral species correlation matrix. In this way, the Mantel test is a multivariate, nonparametric equivalent of an ANOVA that tests whether the among-category distances are greater than the within-category distances (Sokal and Rohlf 1995).

All statistical analyses were conducted using R (ver. 2.3.1; R Development Core Team 2006). Mantel tests used the APE package for R (Paradis et al. 2006).

Empirical Results

Frequency of Coinfection

Our model results suggest that high levels of coinfection occur when cross-protection and synergistic mortality are relatively weak and vectors are abundant, particularly generalist vectors. Of the 1,570 hosts we assayed for B/CYDV, 17% tested positive for at least one species of B/CYDV, and 70% of the infected hosts were infected by multiple viruses (fig. 5). We tested whether this coinfection rate was higher than expected at random by comparing the real frequency distribution of viruses per host with the distribution from 999 random permutations of the virus occurrence data. The real data had a significantly lower frequency of single infected hosts and many more hosts with two or more viral species than expected in random distributions. Of the coinfected hosts, 28% had more than two viruses, a level of coinfection never found in the randomized data (fig. 5).

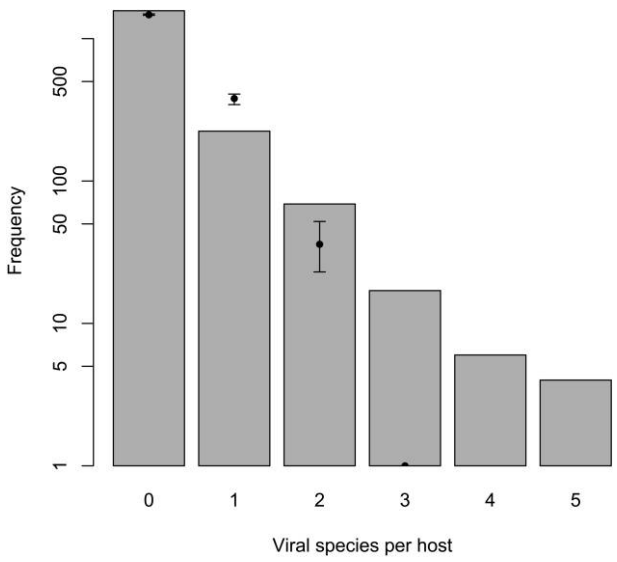

Figure 5: Frequency of multiple infections of barley yellow dwarf virus in the total data set. Circles and error bars represent the mean and range of frequencies in 999 random permutations of the prevalence data.

Temporal Variability of Coinfection

Our model results suggest that viruses sharing a vector should be positively correlated if vector affinity is an important driver of coinfection, while viruses within a viral group should be negatively correlated if synergistic mortality and cross-protection are strongly limiting coinfection. Temporal variability in the B/CYDV community was strongly correlated with vector affinity but was unrelated to viral group (table 2). There was roughly a threefold increase in overall B/CYDV prevalence over the 4-year period covered by this study (fig. 6). This increase in prevalence is closely tracked by the spread of viruses vectored by the generalist *Rhopalosiphum padi* (BYDV-PAV and CYDV-RPV; $r = 0.477$; table 1). In contrast, viruses carried by either of the specialists, *Rhopalosiphum maidis* or *Schizaphis graminum* (BYDV-SGV and CYDV-RMV), were generally constant or declined throughout this period (fig. 6). We present Mantel tests of among-virus correlations among individual hosts, sampled in multiple plots across several years. For this reason, there is a spatial component in these results arising from correlations among hosts in different plots within a year. This effect can be eliminated by basing the Mantel test on the mean prevalence among all hosts collected within a single year. Analysis of yearwise means ($N = 4$) gives comparable results to the host-level analysis; there is no effect of viral group, but there is a strong correlation among viruses carried by *R. padi* (BYDV-PAV and CYDV-RPV).

Spatial Variability of Coinfection

Our model predictions for spatial variability are concordant with those for temporal variability; viruses sharing a vector should be positively correlated, while viruses within a viral group should be negatively correlated. As with temporal variability, spatial variability in the B/CYDV community was strongly correlated with vector affinity but was unrelated to viral group (table 2). While there was little difference in overall prevalence among our three study sites, the viruses carried by *Sitobion avenae* and *Metopolophium dirhodum* (BYDV-MAV and BYDV-PAV; $r = 0.742$; table 1) and viral species vectored by *R. padi* (BYDV-PAV and CYDV-RPV; $r = 0.577$; table 1) showed parallel responses (Hastings > Sedgwick > McLaughlin; fig. 7).

The nested nature of the spatial sampling provides further insight into the relevant spatial scale of the processes governing coinfection rates. There are no significant effects of viral group on among-virus correlations, if we base our Mantel tests on plot means ($N = 9$) or reserve means

Table 2: Results of Mantel tests comparing viral species covariance with an overall vector distance matrix, *Rhopalosiphum padi* virus matrix, *Sitobion avenae*/*Metopolophium dirhodum* virus matrix, and viral group (I BYDV vs. II CYDV) matrix

Location	Years	Vector	*Rhopalosiphum padi*	*Sitobion avenae*/*Metopolophium dirhodum*	Viral group
Cross-site	2005	.001	.091	.001	.902
Sedgwick	2002–2005	.001	.001	.295	.293

Note: Comparisons for the host *Elymus glaucus* are shown for three sites in a single year (cross-site) and for multiple years at a single site.

($N = 3$) as opposed to individual hosts, as presented above. Vector affinity remains highly significant at all three spatial scales (host, plot, and site). Furthermore, overall virus diversity is concordant at all spatial scales. Figure 8 shows the number of viral species at each reserve and the mean number of viral species per population and per individual host in a population. The parallel response in diversity at all scales (Hastings > Sedgwick > McLaughlin) suggests that the number of viruses in an individual host is closely tied to the number of viruses present at large spatial scales (e.g., a reserve).

Discussion

While often overlooked, interactions among pathogens can dramatically influence overall pathogen dynamics. Our modeling results indicate that overall infection prevalence will be highest when there are abundant generalist vectors present in a community and when among-pathogen interactions do not cause strong cross-protection or synergistic mortality. If cross-protection can provide partial immunity for distantly related pathogens, then a greater suite of pathogens will preempt one another within hosts, thereby reducing overall prevalence. At the other extreme, infection prevalence can decline when coinfection results in substantial synergistic host mortality.

From both our model and field results, we predict that pathogens transmitted by abundant shared generalist vectors will tend to have high rates of coinfection, while those carried by specialist vectors will have lower rates of both overall prevalence and coinfection. For example, despite broadly similar geographic ranges, coinfection of malaria (generally vectored by *Anopheles* mosquitoes) and dengue (generally vectored by *Aedes* mosquitoes) is not as common as it could be if they shared mosquito vectors (Knols and Louis 2006).

Our model provides a framework within which we can interpret data on coexisting pathogens in natural systems. Our modeling work suggests that cross-protection and coinfection-induced mortality will lead to low overall coinfection rates and negative correlations among closely related pathogens that preempt one another for hosts. In contrast, our field studies of five coexisting species of B/CYDV revealed a very high level of coinfection and no negative correlations within viral groups that have been shown to cross-protect infected hosts (Miller and Rasochova 1997). These results, taken together, suggest that the laboratory findings of strong within-host viral interactions between viruses from the BYDV and CYDV groups do not produce effective predictions for the field setting and that within-host interactions are relatively weak in natural populations.

Our model also predicted that pathogens sharing a vector should have higher coinfection rates than pathogens carried by separate specialist vectors. Our empirical data were concordant with this prediction. We found that the spatial and temporal correlational structure of the viral community matched the matrix of shared vector affinities (table 1). The spatial correlation was strongest among *S. avenae* and *M. dirhodum* vectored viruses, such that prevalence of BYDV-MAV and BYDV-PAV was highest at our middle-latitude site (Hastings). The *R. padi* vectored viruses (BYDV-PAV and CYDV-RPV) showed a similar, though weaker, association. In contrast, temporal correlations were strongest among *R. padi* vectored viruses. This correlation resulted from a synchronous detection and increase in both BYDV-PAV and CYDV-RPV that were both undetected during the first 2 years of the study. Our examination of coinfection rates at nested spatial scales provides further support for the importance of large-scale processes in determining coinfection rates. Within-host rates of coinfection closely mirrored large-scale patterns of pathogen diversity.

While our primary goal has been to investigate processes controlling coinfection in the suite of BYD and CYD viruses, our data show interesting changes in overall prevalence. B/CYDV prevalence has been reported to increase in the presence of annual grasses or irrigated fields; during cool, moist, prolonged growing seasons; and in older perennial grass swards (Dempster and Holmes 1995; Hewings and Eastman 1995; Malmstrom et al. 2005*a*; Borer et al. 2007). We did not observe any systematic variability in annual grass abundance among years or across our study sites, and rainfall patterns did not match patterns of virus

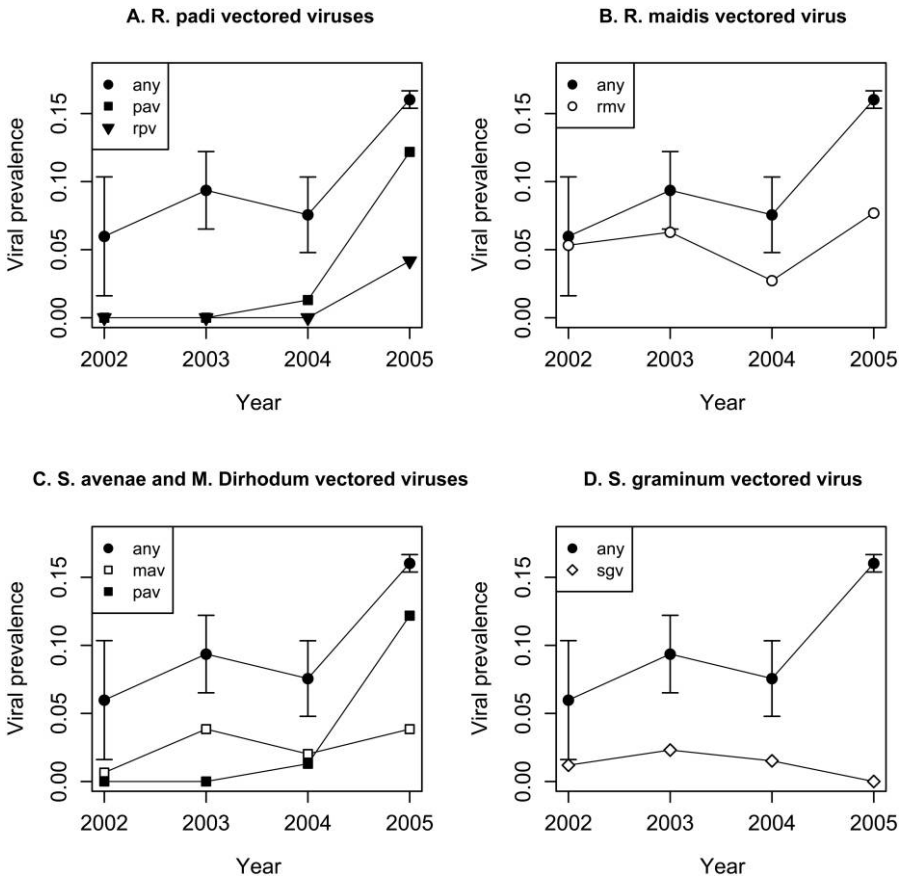

Figure 6: Change in overall prevalence of five barley and cereal yellow dwarf viruses in *Elymus glaucus* at Sedgwick Reserve in four consecutive years. Total prevalence (infection by any of the five viruses [*any*]) is also included. The four graphs show viruses carried by subsets of the vector community.

prevalence (see site description for rainfall data). We did observe a threefold increase in overall prevalence from 2002 to 2005 at our Sedgwick sites (fig. 6). These samples were collected in a restored grassland planted in 1998, and so it is possible that this increase was driven by the same process observed by Dempster and Holmes (1995), with prevalence increasing with field age.

Our model focused on interactions among species of a single pathogen type, in which the relative strengths of cross-protection and synergistic mortality switch in importance as species become increasingly unique. This is a common phenomenon in viral pathogens. We can examine the more general case, in which cross-protection (ψ) and synergistic mortality (μ_2) are completely independent, by removing ψ from the death rate of equation (4). In this type of system, synergistic mortality either does not occur at all ($\mu_2 = 0$) or occurs even when there is cross-protection ($\mu_2 > 0$ for all ψ). Both cases lack compensation between cross-protection and synergistic mortality, so the pathogen prevalence increases as cross-protection declines ($\psi = 1$; fig. 4). Thus, a complex of fully unique pathogens will obtain higher overall prevalence than a complex of more closely related pathogens.

Our model illustrates the interaction between three specific mechanisms of ecological interference among coexisting pathogens (sensu Rohani et al. 2003): cross-protection, coinfection-induced virulence, and coinfection-reduced transmission. These interference mechanisms have been demonstrated in many animal (Lal et al. 1994; Kamal et al. 2001*a*, 2001*b*) and plant (Gildow and Rochow 1980; Gray et al. 1991; Wen et al. 1991; Power 1996; Miller and Rasochova 1997; Hood 2003; Al-Naimi et al. 2005) pathogen systems and can have important consequences for the ecology of multipathogen systems. However, we find that processes occurring at broad spatial and temporal scales may be more important in natural systems, where, unlike many diseases of humans, single host–single vector interactions are relatively rare.

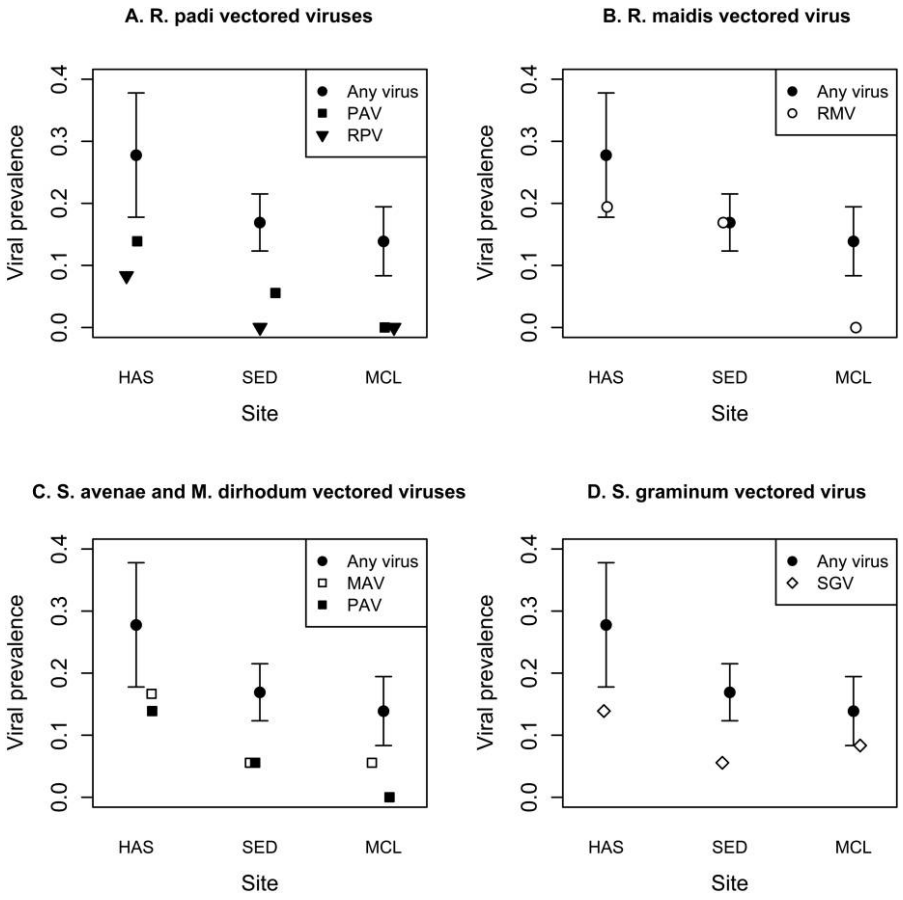

Figure 7: Change in overall prevalence of five barley and cereal yellow dwarf viruses in *Elymus glaucus* at three reserves in California: Hastings (*HAS*), Sedgwick (*SED*), and McLaughlin (*MCL*). Total prevalence (infection by any of the five viruses [*any*]) is also included. The four graphs show viruses carried by subsets of the vector community.

Although our modeling work was motivated by a specific plant-pathogen system, many of our results are likely general to other plant and animal pathogen communities. Plants and animals have evolved both constitutive and inducible defenses, and innate pathogen responses are mechanistically similar across most kingdoms (Harvell 1990; Soosaar et al. 2005; Jones and Dangl 2006). Vertebrates are distinctive from other hosts in having evolved adaptive immunity and mobile defender cells that can confer long-term immunity to specific pathogens (Harvell 1990; Jones and Dangl 2006). This would involve several issues that we do not examine here, namely, recovery from infection and long-lasting immunity; these factors would be most important for diseases where cross-protection is strong and have been the focus of research for many human diseases (Hall et al. 1991; Ferguson et al. 1999; Bjornstad et al. 2002; Adams et al. 2006; Wearing and Rohani 2006). Our current model does not examine long latent periods or seasonality, although we have done so in earlier work (Borer et al. 2007). All of these factors can be important, particularly in concert, and could create long-term cycles in pathogen dynamics (Altizer et al. 2006).

Unfortunately, we have relatively short-term, coarse-scale data on the temporal pattern of B/CYDV in California grasslands (fig. 6), and we could not detect any particular dynamical signature. Given the lack of a strong, adaptive immune response, we would not expect multiannual cycles of disease (cf. Bjornstad et al. 2002; Rohani et al. 2003), although we expect a seasonal transmission signal to cause seasonal dynamics (cf. Hosseini et al. 2004). We do, however, expect that our results will hold for long-term averages for other more complex systems but will not provide insight into the temporal complexities that can occur when seasonal transmission and host biology interact with immune function. Therefore, we focus on an equilibrium analysis to give us broad insight into regional patterns and, in particular, to contrast the forces of vector specialization and abundance with within-host forces at

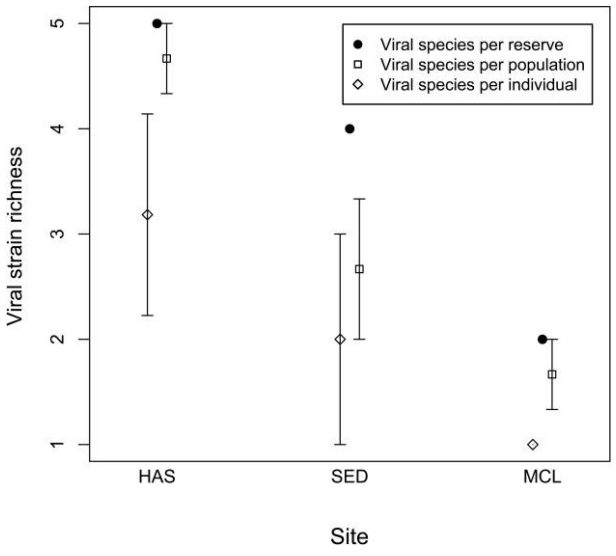

Figure 8: Spatial variability in viral richness in *Elymus glaucus* at three reserves in California: Hastings (*HAS*), Sedgwick (*SED*), and McLaughlin (*MCL*). Number of viral species are shown at three spatial scales: viral species per reserve (*circles*), viral species per population at a reserve (*squares*), and viral species per host in a single population (*diamonds*).

broad scales. These general aspects of many disease systems remain similar across kingdoms—host immunity contrasted with vector and host community dynamics—and although complex temporal dynamics would likely complicate this picture, they are unlikely to remove the strong effects of the vector community that we find here.

We have little information on the actual seasonality of aphid vector dynamics in California, although it can be important (Carter et al. 1982). Previous work has shown that seasonality does affect the community composition and temporal dynamics of B/CYDV in California grasslands (Borer et al. 2007). Thus, we expect that a more complex view of the dynamics of this system will develop as we deepen our understanding of the seasonal forces in this system, in particular, the role of vectors in controlling disease prevalence and coinfection.

Our results have important implications for ecological facilitation among coexisting pathogens through increased transmission when heterologous encapsidation allows pathogens to increase their suite of efficient vector species (Rochow 1970*b*; Creamer and Falk 1990). We predict that this transcapsidation process should increase prevalence and coinfection by increasing transmission and making any specialist vector species in the system become more like generalists. Facilitation also can occur when initial infections lower host resistance (Bentwich et al. 1999; Tirado and Yoon 2003; Koskella et al. 2006), as is seen in immunodeficiency syndromes and cross-regulated immune systems for micro- and macroparasites (Bentwich et al. 1999; Yazdanbakhsh et al. 2002; Coico et al. 2003; Jolles et al. 2008). Finally, facilitation can arise directly when one virus increases the replication rate of a second invading virus (e.g., antibody-dependent enhancement, as in Montefiori et al. 1996; Ferguson et al. 1999; Tirado and Yoon 2003). The link between pathogen communities and the well-developed ecological literature on positive interactions (e.g., Bertness and Leonard 1997; Loreau and Hector 2001; Halpern et al. 2007) is an area that has been little explored but is likely to be fruitful.

In our work, we have focused on the interactions among pathogens simultaneously cohabiting a single host. Strict coinfection is a subset of a larger and more complex suite of ways in which pathogens can interact to alter host and pathogen vital rates. For example, infection by a single pathogen can alter the host-pathogen interactions governing subsequent infections, although the two pathogens do not coexist within a single host. A fascinating example of these types of interactions is dengue, a viral pathogen in which interactions among serotypes are governed by complex time lags in immunological responses. Infection by a single strain confers transient cross-protection against other serotypes. However, infection by a second serotype following this period of cross-protection results in much more severe symptoms as a result of antibody-dependent enhancement (Hall et al. 1991; Ferguson et al. 1999; Adams et al. 2006; Wearing and Rohani 2006). Dengue is also of particular relevance to the B/CYDV system, because pathogen dynamics arise from within-host processes, environmental factors, and vector dynamics (Wearing and Rohani 2006; Alto et al. 2008).

Interactions among pathogens can alter disease dynamics by altering vital rates such as transmission and mortality (Rochow 1970*b*; Creamer and Falk 1990; Montefiori et al. 1996; Miller and Rasochova 1997; Rohani et al. 2003; Lello et al. 2004; Koskella et al. 2006; Pedersen and Fenton 2007); however, few studies have examined among-pathogen interactions in free-living hosts, and those few have focused on within-host interactions (Lello et al. 2004; Jolles et al. 2008). We have demonstrated that the distribution of five coexisting viral pathogens in naturally occurring hosts is well described by vector affinity and broadscale spatial processes. Our field system does not provide a unique case; we expect that the composition of many pathogen communities is molded by interactions and processes external to individual hosts. Given that more than 80% of the world's high-priority emerging diseases are vector transmitted (Millennium Ecosystem Assessment 2005), this work is a first step in developing a deeper understanding of the ways in which vector and pathogen community interactions control both spatial and temporal infection dynamics.

Acknowledgments

K. Blaisdell, A. Borcher, G. Creager, C. Kahlke, L. Neys, J. Quinn, and T. Yoshida were invaluable in collecting and assembling the data used in this manuscript. A. E. Jolles provided useful comments on an earlier version of this manuscript. We greatly appreciate the thoughtful comments from three anonymous reviewers. Support for this project was provided in part by U.S. Department of Agriculture National Research Initiative Competitive Grants Program 2003-35316-13767 (to C. Briggs and E.T.B.), National Science Foundation (NSF) DEB 02-35624 (to O. Reichman, E.W.S., and J. Schimel), Cornell University (to A.G.P.), NSF DEB-0444639 (to A.G.P. and C. Mitchell), and NSF/National Institutes of Health Ecology of Infectious Diseases 05-25666 (to E.T.B., A. Dobson, P.R.H., C. Mitchell, A.G.P., and E.W.S.).

APPENDIX A

Supplemental Tables and Figures

Table A1: Parameter values for two-pathogen model (eq. [1])

Parameter	Default value	Meaning
β_V	.04	Transmission rate from vectors to plants
$\beta_{Z,C}$	.04	Virus acquisition from plants by vector species Z of pathogen C
b_S	45.00	Birth rate for susceptibles
b_1	22.50	Birth rate for infecteds
b_2	11.25	Birth rate for coinfecteds
K	100.00	Density-dependent mortality factor
μ_0	.13	Background mortality
μ_1	.13	Disease-induced mortality
μ_2	.13	Synergistic mortality
ψ	.50	Pathogen taxa similarity
δ	12	Aphid mortality rate

Note: Parameters based on Seabloom et al. (2003), Malmstrom et al. (2005*b*), and Borer et al. (2007).

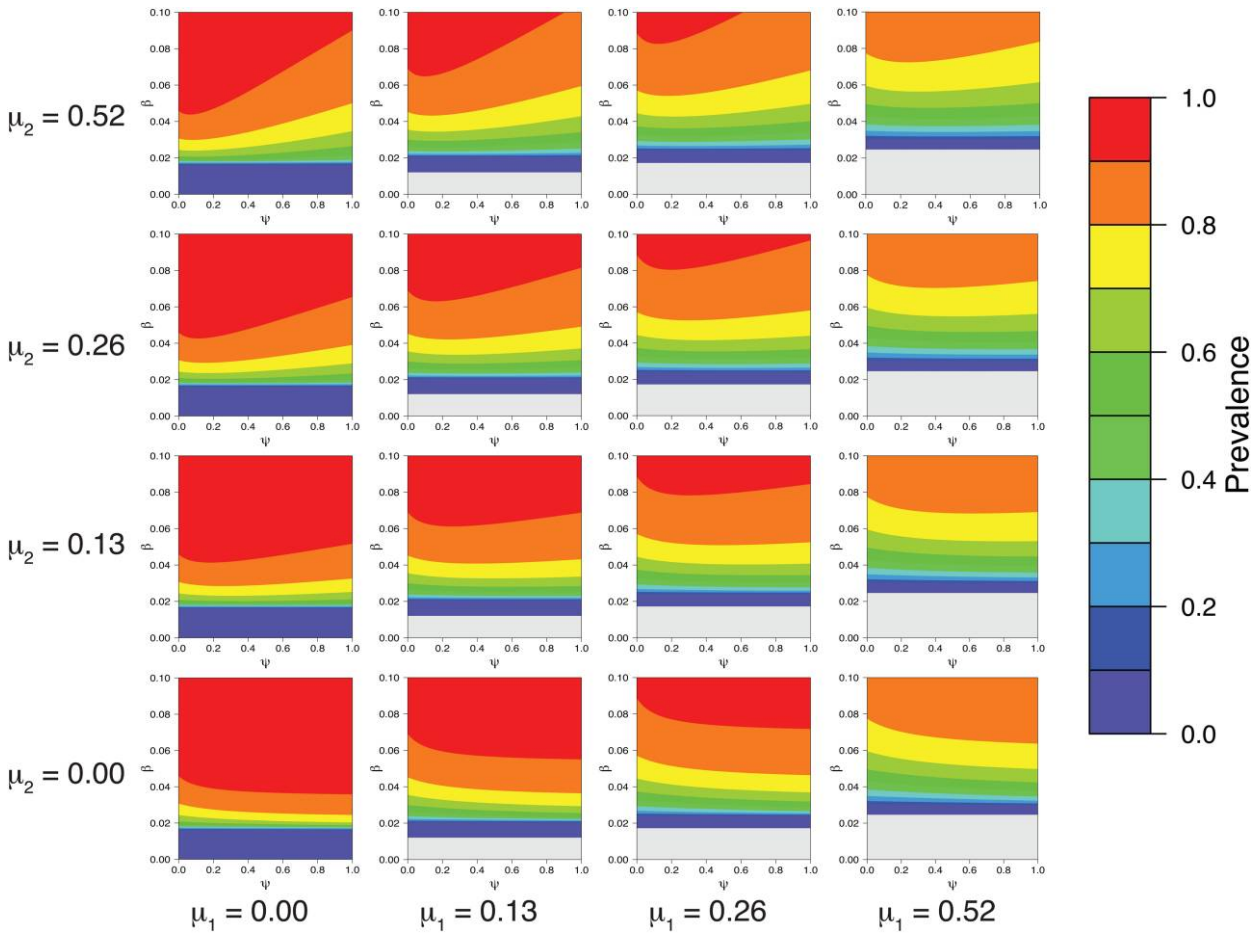

Figure A1: Total prevalence as a combined function of transmission (β) and pathogen similarity (ψ) for four values of disease-induced mortality (μ_1 and μ_2) for a system with a single generalist vector ($X = 100$, $Y = 0$). Other parameters as in table A1.

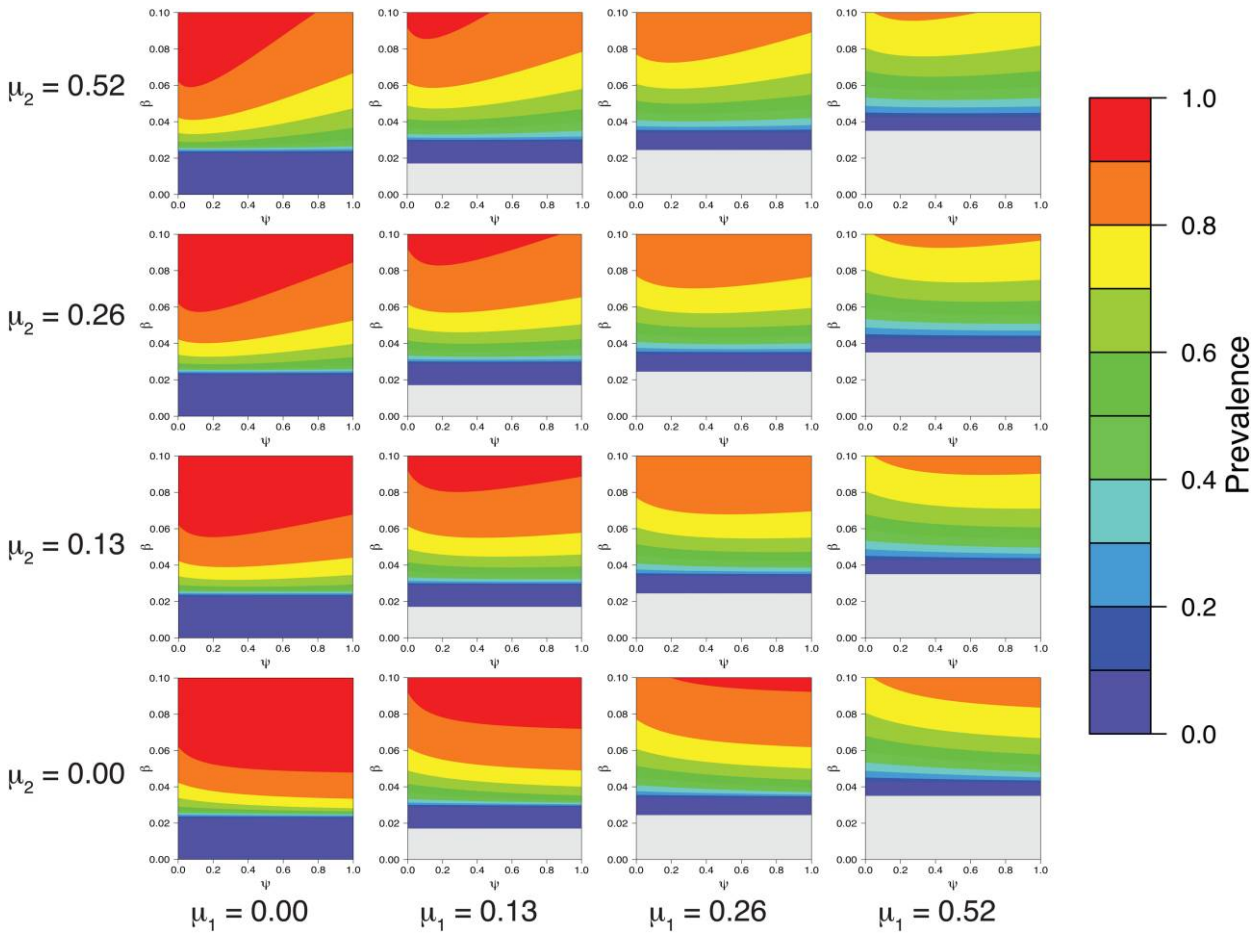

Figure A2: Total prevalence as a combined function of transmission (β) and pathogen similarity (ψ) for four values of disease-induced mortality (μ_1 and μ_2) for a system with two specialist vectors ($X = 50, Y = 50$). White areas represent parameter values for which the disease cannot persist. Other parameters as in table A1.

APPENDIX B

Vector Pseudoequilibrium

We seek to include multiple vector species in our model of multipathogen disease dynamics but avoid the complexities of (at least) four additional dynamical equations. Particularly for systems such as B/CYDVs, where no replication occurs in the vector, a separation of timescales argument should be reasonable and successful. Therefore, we solve for the pseudoequilibrium of viruliferous aphids, given a fixed aphid population. We fix our aphid population at size Z, for simplicity, and because aphids are often regulated by external factors such as generalist predators and seasonality. We designate uninfected vectors as U, exposed vectors as E, and infected, or viruliferous, aphids as V. The per capita rate of the aphid visitation is ν, the probability of virus acquisition is φ, background mortality is δ, and I represents the number of infected plants.

This gives an equation for the rate of change of exposed and viruliferous aphids:

$$\frac{dE}{dt} = \nu\phi IU - \gamma E,$$

$$\frac{dV}{dt} = \gamma E - \delta V.$$

We then solve for the equilibrium value of exposed aphids as a function of viruliferous aphids:

$$0 = \gamma E - \delta V \rightarrow E = \frac{\delta}{\gamma} V.$$

We then solve for the equilibrium value of viruliferous aphids:

$$\begin{aligned} 0 &= \nu\phi IU - \gamma E \\ &= \nu\phi I[Z - (E + V)] - \gamma E \\ &= \nu\phi I\left[Z - \left(\frac{\delta}{\gamma} V + V\right)\right] - \delta V \\ &= \nu\phi IZ - \nu\phi I\frac{\delta}{\gamma} V - \nu\phi IV - \delta V \\ &= \nu\phi IZ - V\left(\nu\phi\frac{\delta}{\gamma} I + \nu\phi I + \delta\right), \\ V^* &= \frac{\nu\phi I}{\nu\phi I + \nu\phi(\delta/\gamma)I + \delta} Z. \end{aligned}$$

As the latent/exposed period shrinks, γ goes to infinity, and thus the middle term disappears from the denominator. Because B/CYDV has a very short exposed period ($36{,}000 > \gamma > 100$), we will ignore this term from now on.

We now have the (pseudo)equilibrium number of viruliferous aphids for a single pathogen and a single vector. Table B1 shows the possible interactions when two vector species carry two pathogens; ν_Z is visitation rate of vector species X or Y, and $\varphi_{Z,C}$ is the probability of vector Z acquiring pathogen C, where pathogens are A or B. (There is the $(1 - \varphi_{Z,A})(1 - \varphi_{Z,B})$ set of interactions, but they do not lead to viruliferous aphids.) "Pathogen vector" refers to vectors by pathogen carried rather than by species.

Unless the vector species are specialists and $\varphi_{X,B} = \varphi_{Y,A} = 0$, the vector species and pathogen vectors are very different groupings. If we define $\beta_{Z,C} = \nu_Z \times \varphi_{Z,C}$, and solve for pseudoequilibrium, we can obtain the following pathogen by species viruliferous vector abundances:

$$V_{X,A} = \frac{\beta_{X,A}(I_A + I_{A,B})}{\beta_{X,A}(I_A + I_{A,B}) + \beta_{X,B}(I_B + I_{A,B}) + \delta} X,$$

$$V_{X,B} = \frac{\beta_{X,B}(I_A + I_{A,B})}{\beta_{X,A}(I_A + I_{A,B}) + \beta_{X,B}(I_B + I_{A,B}) + \delta} X,$$

$$V_{Y,A} = \frac{\beta_{Y,A}(I_A + I_{A,B})}{\beta_{Y,A}(I_A + I_{A,B}) + \beta_{Y,B}(I_B + I_{A,B}) + \delta} Y,$$

$$V_{Y,B} = \frac{\beta_{Y,B}(I_A + I_{A,B})}{\beta_{Y,A}(I_A + I_{A,B}) + \beta_{Y,B}(I_B + I_{A,B}) + \delta} Y.$$

Reducing to just pathogen vectors, we obtain

$$V_{\mathrm{A}} = \frac{\beta_{\mathrm{X,A}}(I_{\mathrm{A}} + I_{\mathrm{A,B}})}{\beta_{\mathrm{X,A}}(I_{\mathrm{A}} + I_{\mathrm{A,B}}) + \beta_{\mathrm{X,B}}(I_{\mathrm{B}} + I_{\mathrm{A,B}}) + \delta} X + \frac{\beta_{\mathrm{Y,A}}(I_{\mathrm{A}} + I_{\mathrm{A,B}})}{\beta_{\mathrm{Y,A}}(I_{\mathrm{A}} + I_{\mathrm{A,B}}) + \beta_{\mathrm{Y,B}}(I_{\mathrm{B}} + I_{\mathrm{A,B}}) + \delta} Y,$$

$$V_{\mathrm{B}} = \frac{\beta_{\mathrm{X,B}}(I_{\mathrm{A}} + I_{\mathrm{A,B}})}{\beta_{\mathrm{X,A}}(I_{\mathrm{A}} + I_{\mathrm{A,B}}) + \beta_{\mathrm{X,B}}(I_{\mathrm{B}} + I_{\mathrm{A,B}}) + \delta} X + \frac{\beta_{\mathrm{Y,B}}(I_{\mathrm{A}} + I_{\mathrm{A,B}})}{\beta_{\mathrm{Y,A}}(I_{\mathrm{A}} + I_{\mathrm{A,B}}) + \beta_{\mathrm{Y,B}}(I_{\mathrm{B}} + I_{\mathrm{A,B}}) + \delta} Y,$$

which is equation (5). Then we can simply consider pathogen vectors as a function of total possible vector abundance without a loss of generality. We now have a pathogen-vector transmission matrix:

$$\beta = \begin{bmatrix} \beta_{\mathrm{X,A}} & \beta_{\mathrm{X,B}} \\ \beta_{\mathrm{Y,A}} & \beta_{\mathrm{Y,B}} \end{bmatrix}.$$

If the vectors are generalists, all entries are positive, although this can be caused by variation in either aphid visitation (ν_Z) or efficiency ($\phi_{\mathrm{Z,C}}$). It would also be straightforward to expand this to include multiple hosts and host preferences. In the case of specialist vectors, the matrix reduces to the diagonal:

$$\beta = \begin{bmatrix} \beta_{\mathrm{X,A}} & 0 \\ 0 & \beta_{\mathrm{Y,B}} \end{bmatrix},$$

where $\beta_{\mathrm{X,B}} = \beta_{\mathrm{Y,A}} = 0$.

Table B1: Possible interactions leading to two vector species carrying two pathogens, allowing for mixed carrying of pathogens

	Vector species	Plant	Acquisition rate	Pathogen vector
1	V_{X}	I_{A}	$\nu_{\mathrm{X}}\phi_{\mathrm{X,A}}XI_{\mathrm{A}}$	V_{A}
2	V_{X}	$I_{\mathrm{A,B}}$	$\nu_{\mathrm{X}}\phi_{\mathrm{X,A}}(1-\phi_{\mathrm{X,B}})XI_{\mathrm{A,B}}$	V_{A}
3	V_{X}	$I_{\mathrm{A,B}}$	$\nu_{\mathrm{X}}\phi_{\mathrm{X,A}}\phi_{\mathrm{X,B}}XI_{\mathrm{A,B}}$	V_{A}, V_{B}
4	V_{X}	$I_{\mathrm{A,B}}$	$\nu_{\mathrm{X}}(1-\phi_{\mathrm{X,A}})\phi_{\mathrm{X,B}}XI_{\mathrm{A,B}}$	V_{B}
5	V_{X}	I_{B}	$\nu_{\mathrm{X}}\phi_{\mathrm{X,B}}XI_{\mathrm{B}}$	V_{B}
6	V_{Y}	I_{B}	$\nu_{\mathrm{Y}}\phi_{\mathrm{Y,B}}YI_{\mathrm{B}}$	V_{B}
7	V_{Y}	$I_{\mathrm{A,B}}$	$\nu_{\mathrm{Y}}\phi_{\mathrm{Y,B}}(1-\phi_{\mathrm{Y,A}})YI_{\mathrm{A,B}}$	V_{B}
8	V_{Y}	$I_{\mathrm{A,B}}$	$\nu_{\mathrm{Y}}\phi_{\mathrm{Y,B}}\phi_{\mathrm{Y,A}}YI_{\mathrm{A,B}}$	V_{A}, V_{B}
9	V_{Y}	$I_{\mathrm{A,B}}$	$\nu_{\mathrm{Y}}(1-\phi_{\mathrm{Y,B}})\phi_{\mathrm{Y,A}}YI_{\mathrm{A,B}}$	V_{A}
10	V_{Y}	I_{A}	$\nu_{\mathrm{Y}}\phi_{\mathrm{Y,A}}YI_{\mathrm{A}}$	V_{A}

Literature Cited

Adams, B., E. C. Holmes, C. Zhang, M. P. Mammen, S. Nimmannitya, S. Kalayanarooj, and M. Boots. 2006. Cross-protective immunity can account for the alternating epidemic pattern of dengue virus serotypes circulating in Bangkok. Proceedings of the National Academy of Sciences of the USA 103:14234–14239.

Agrios, G. N. 1988. Plant pathology. Academic Press, Orlando, FL.

Al-Naimi, F. A., K. A. Garrett, and W. W. Bockus. 2005. Competition, facilitation, and niche differentiation in two foliar pathogens. Oecologia (Berlin) 143:449–457.

Altizer, S., A. Dobson, P. Hosseini, P. Hudson, M. Pascual, and P. Rohani. 2006. Seasonality and the dynamics of infectious disease. Ecology Letters 9:467–484.

Alto, B. W., L. P. Lounibos, C. N. Mores, and M. H. Reiskind. 2008. Larval competition alters susceptibility of adult aedes mosquitoes to dengue infection. Proceedings of the Royal Society B: Biological Sciences 275:463–471.

Bentwich, Z., A. Kalinkovich, Z. Weisman, G. Borkow, N. Beyers, and A. D. Beyers. 1999. Can eradication of helminthic infections change the face of AIDS and tuberculosis? Immunology Today 20: 485–487.

Bertness, M. D., and G. H. Leonard. 1997. The role of positive interactions in communities: lessons from intertidal habitats. Ecology 78:1976–1989.

Bjornstad, O. N., B. F. Finkenstadt, and B. T. Grenfell. 2002. Dynamics of measles epidemics: estimating scaling of transmission rates using a time series SIR model. Ecological Monographs 72: 169–184.

Borer, E. T., P. R. Hosseini, E. W. Seabloom, and A. P. Dobson. 2007. Pathogen-induced reversal of native perennial dominance in a

grassland community. Proceedings of the National Academy of Sciences of the USA 104:5473–5478.

Carter, N., A. F. G. Dixon, and R. Rabbinge. 1982. Cereal aphid populations: biology, simulation and prediction. Pudoc, Wageningen.

Coico, R., G. Sunshine, and E. Benjamini. 2003. Immunology: a short course. 5th ed. Wiley-Liss, Hoboken, NJ.

Creamer, R., and B. W. Falk. 1990. Direct detection of transcapsidated barley yellow dwarf luteoviruses in double infected plants. Journal of General Virology 71:211–217.

Cumming, G. S., and J. F. Guegan. 2006. Food webs and disease: is pathogen diversity limited by vector diversity? Ecohealth 3:163–170.

D'Antonio, C. M., and P. M. Vitousek. 1992. Biological invasions by exotic grasses, the grass/fire cycle, and global change. Annual Review of Ecology and Systematics 23:63–87.

D'Arcy, C. 1995. Symptomology and host range of barley yellow dwarf. Pages 9–28 *in* C. D'Arcy and P. Burnett, eds. Barley yellow dwarf: 40 years of progress. American Phytopathological Society, St. Paul, MN.

Dempster, L. C., and S. J. I. Holmes. 1995. The incidence of strains of barley yellow dwarf virus in perennial ryegrass crops in southwest and central Scotland. Plant Pathology 44:710–717.

Durrant, W. E., and X. Dong. 2004. Systemic acquired resistance. Annual Review of Phytopathology 42:185–209.

Ferguson, N., R. Anderson, and S. Gupta. 1999. The effect of antibody-dependent enhancement on the transmission dynamics and persistence of multiple-strain pathogens. Proceedings of the National Academy of Sciences of the USA 96:790–794.

Gildow, F. E., and W. F. Rochow. 1980. Transmission interference between two isolates of barley yellow dwarf virus in *Macrosiphum avenae*. Phytopathology 70:122–126.

Gray, S. M., A. G. Power, D. M. Smith, A. J. Seaman, and N. S. Altman. 1991. Aphid transmission of barley yellow dwarf virus: acquisition feeding periods and virus concentration requirements. Phytopathology 81:539–545.

Halbert, S., and D. Voegtlin. 1995. Biology and taxonomy of vectors of barley yellow dwarf viruses. Pages 217–258 *in* C. D'Arcy and P. Burnett, eds. Barley yellow dwarf: 40 years of progress. American Phytopathological Society, St. Paul, MN.

Hall, W. C., T. P. Crowell, D. M. Watts, V. L. R. Barros, H. Kruger, F. Pinheiro, and C. J. Peters. 1991. Demonstration of yellow fever and dengue antigens in formalin-fixed paraffin-embedded human liver by immunohistochemical analysis. American Journal of Tropical Medicine and Hygiene 45:408–417.

Halpern, B. S., B. R. Silliman, J. D. Olden, J. P. Bruno, and M. D. Bertness. 2007. Incorporating positive interactions in aquatic restoration and conservation. Frontiers in Ecology and the Environment 5:153–160.

Harvell, C. D. 1990. The ecology and evolution of inducible defenses. Quarterly Review of Biology 65:323–340.

Heady, H. F. 1977. Valley grassland. Pages 491–514 *in* M. G. Barbour and J. Major, eds. Terrestrial vegetation of California. Wiley, New York.

Hewings, A. D., and C. E. Eastman. 1995. Epidemiology of barley yellow dwarf in North America. Pages 75–106 *in* C. D'Arcy and P. Burnett, eds. Barley yellow dwarf: 40 years of progress. American Phytopathological Society, St. Paul, MN.

Hood, M. E. 2003. Dynamics of multiple infection and within-host competition by the anther-smut pathogen. American Naturalist 162:122–133.

Hosseini, P. R., A. A. Dhondt, and A. Dobson. 2004. Seasonality and wildlife disease: how seasonal birth, aggregation and variation in immunity affect the dynamics of *Mycoplasma gallisepticum* in house finches. Proceedings of the Royal Society B: Biological Sciences 271:2569–2577.

Huang, Y., and P. Rohani. 2005. The dynamical implications of disease interference: correlations and coexistence. Theoretical Population Biology 68:205–215.

Irwin, M. E., and J. M. Thresh. 1990. Epidemiology of barley yellow dwarf: a study in ecological complexity. Annual Review of Phytopathology 28:393–424.

Jensen, S. G., and C. D'Arcy. 1995. Effects of barley yellow dwarf on host plants. Pages 55–74 *in* C. D'Arcy and P. Burnett, eds. Barley yellow dwarf: 40 years of progress. American Phytopathological Society, St. Paul, MN.

Jolles, A. E., V. O. Ezenwa, R. S. Etienne, W. C. Turner, and H. Olff. 2008. Interactions between macroparasites and microparasites drive infection patterns in free-ranging African buffalo. Ecology 89:2239–2250.

Jones, J. D. G., and J. L. Dangl. 2006. The plant immune system. Nature 444:323–329.

Kamal, S. M., J. W. Rasenack, L. Bianchi, A. Al Tawil, K. E. S. Khalifa, T. Peter, H. Mansour, W. Ezzat, and M. Koziel. 2001*a*. Acute hepatitis C without and with schistosomiasis: correlation with hepatitis C-specific CD4(+) T-cell and cytokine response. Gastroenterology 121:646–656.

Kamal, S. M., L. Bianchi, A. Al Tawil, M. Koziel, K. E. Khalifa, T. Peter, and J. W. Rasenack. 2001*b*. Specific cellular immune response and cytokine patterns in patients coinfected with hepatitis C virus and *Schistosoma mansoni*. Journal of Infectious Diseases 184:972–982.

Knols, B., and C. Louis, eds. 2006. Bridging laboratory and field research for genetic control of disease vectors. Springer, Dordrecht.

Koskella, B., T. Giraud, and M. E. Hood. 2006. Pathogen relatedness affects the prevalence of within-host competition. American Naturalist 168:121–126.

Lal, R. B., D. Rudolph, M. P. Alpers, A. J. Sulzer, Y. P. Shi, and A. A. Lal. 1994. Immunologic cross-reactivity between structural proteins of human T-cell lymphotropic virus type I and the blood stage of *Plasmodium falciparum*. Clinical and Diagnostic Laboratory Immunology 1:5–10.

Leclercq-Le Quillec, F., M. Plantegenest, G. Riault, and C. A. Dedryver. 2000. Analyzing and modeling temporal disease progress of barley yellow dwarf virus serotypes in barley fields. Phytopathology 90:860–866.

Lello, J., B. Boag, A. Fenton, I. R. Stevenson, and P. J. Hudson. 2004. Competition and mutualism among the gut helminths of a mammalian host. Nature 428:840–844.

Loreau, M., and A. Hector. 2001. Partitioning selection and complementarity in biodiversity experiments. Nature 412:72–76.

MacDonald, G. 1957. The epidemiology and control of malaria. Oxford University Press, Oxford.

Malmstrom, C. M., and R. Shu. 2004. Multiplexed RT-PCR for streamlined detection and separation of barley and cereal yellow dwarf viruses. Journal of Virological Methods 120:69–78.

Malmstrom, C. M., A. J. McCullough, H. A. Johnson, L. A. Newton, and E. T. Borer. 2005*a*. Invasive annual grasses indirectly increase virus incidence in California native perennial bunchgrasses. Oecologia (Berlin) 145:153–164.

Malmstrom, C. M., C. C. Hughes, L. A. Newton, and C. J. Stoner.

2005*b*. Virus infection in remnant native bunchgrasses from invaded California grasslands. New Phytologist 168:217–230.

Malmstrom, C. M., C. J. Stoner, S. Brandenburg, and L. A. Newton. 2006. Virus infection and grazing exert counteracting influences on survivorship of native bunchgrass seedlings competing with invasive exotics. Journal of Ecology 94:264–275.

May, R. M., and M. A. Nowak. 1995. Coinfection and the evolution of parasite virulence. Proceedings of the Royal Society B: Biological Sciences 261:209–215.

Mensing, S., and R. Byrne. 1998. Pre-mission invasion of *Erodium cicutarium* in California. Journal of Biogeography 25:757–762.

Millennium Ecosystem Assessment. 2005. Ecosystems and human well-being: synthesis. Island, Washington, DC.

Miller, W. A., and L. Rasochova. 1997. Barley yellow dwarf viruses. Annual Review of Phytopathology 35:167–190.

Montefiori, D. C., G. Pantaleo, L. M. Fink, J. T. Zhou, J. Y. Zhou, M. Bilska, G. D. Miralles, and A. S. Fauci. 1996. Neutralizing and infection-enhancing antibody responses to human immunodeficiency virus type 1 in long-term nonprogressors. Journal of Infectious Diseases 173:60–67.

Paradis, E., K. Strimmer, J. Claude, G. Jobb, R. Opgen-Rhein, J. Dutheil, Y. Noel, B. Bolker, and J. Lemon. 2006. APE: analyses of phylogenetics and evolution. R package, version 1.8–3.

Pedersen, A. B., and A. Fenton. 2007. Emphasizing the ecology in parasite community ecology. Trends in Ecology & Evolution 22: 133–139.

Power, A. G. 1996. Competition between viruses in a complex plant-pathogen. Ecology 77:1004–1010.

Power, A. G., and S. M. Gray. 1995. Aphid transmission of barley yellow dwarf viruses: interactions between viruses, vectors, and host plants. Pages 259–289 *in* C. D'Arcy and P. Burnett, eds. Barley yellow dwarf: 40 years of progress. American Phytopathological Society, St. Paul, MN.

Power, A. G., A. J. Seaman, and S. M. Gray. 1991. Aphid transmission of barley yellow dwarf virus: inoculation feeding periods and epidemiological implications. Phytopathology 81:545–548.

R Development Core Team. 2006. R: a language and environment for statistical computing. R Foundation for Statistical Computing, Vienna. http://www.r-project.org.

Rochow, W. F. 1970*a*. Barley yellow dwarf virus. Descriptions of Plant Viruses no. 32. Association of Applied Biology, Kew.

———. 1970*b*. Barley yellow dwarf virus: phenotypic mixing and vector specificity. Science 167:875–878.

———. 1986. Barley yellow dwarf virus. Methods for Enzyme Analysis 11:420–430.

Rohani, P., C. J. Green, N. B. Mantilla-Beniers, and B. T. Grenfell. 2003. Ecological interference between fatal diseases. Nature 422: 885–888.

Seabloom, E. W., A. P. Dobson, and D. M. Stoms. 2002. Extinction rates under nonrandom patterns of habitat loss. Proceedings of the National Academy of Sciences of the USA 99:11229–11234.

Seabloom, E. W., W. S. Harpole, O. J. Reichman, and D. Tilman. 2003. Invasion, competitive dominance, and resource use by exotic and native California grassland species. Proceedings of the National Academy of Sciences of the USA 100:13384–13389.

Sokal, R. R., and F. J. Rohlf. 1995. Biometry: the principles and practice of statistics in biological research. 3rd ed. W. H. Freeman, New York.

Soosaar, J. L. M., T. M. Burch-Smith, and S. P. Dinesh-Kumar. 2005. Mechanisms of plant resistance to viruses. Nature Reviews Microbiology 3:789–798.

Stein, B. A., L. S. Kutner, and J. S. Adams, eds. 2000. Precious heritage: the status of biodiversity in the United States. Oxford University Press, New York.

Thomas, M. B., E. L. Watson, and P. Valverde-Garcia. 2003. Mixed infections and insect-pathogen interactions. Ecology Letters 6:183–188.

Tirado, S. M. C., and K. J. Yoon. 2003. Antibody-dependent enhancement of virus infection and disease. Viral Immunology 16: 69–86.

Wearing, H. J., and P. Rohani. 2006. Ecological and immunological determinants of dengue epidemics. Proceedings of the National Academy of Sciences of the USA 103:11802–11807.

Wen, F., R. M. Lister, and F. A. Fattouh. 1991. Cross-protection among strains of barley yellow dwarf virus. Journal of General Virology 72:791–799.

Woolhouse, M. E. J., C. Dye, J.-F. Etard, T. Smith, J. D. Charlwood, G. P. Garnett, P. Hagan, et al. 1997. Heterogeneities in the transmission of infectious agents: implications for the design of control programs. Proceedings of the National Academy of Sciences of the USA 94:338–342.

Yazdanbakhsh, M., P. G. Kremsner, and R. van Ree. 2002. Immunology: allergy, parasites, and the hygiene hypothesis. Science 296: 490–494.

Zhang, X. S., and J. Holt. 2001. Mathematical models of cross protection in the epidemiology of plant-virus diseases. Phytopathology 91:924–934.

Associate Editor: Pejman Rohani
Editor: Michael C. Whitlock

Grain aphid (*Sitobion avenae*), a vector for barley yellow dwarf viruses, on cultivated oats (*Avena sativa*). Photograph by Mikal Davis.